Four-terminal measurement on a quasi 1D channel

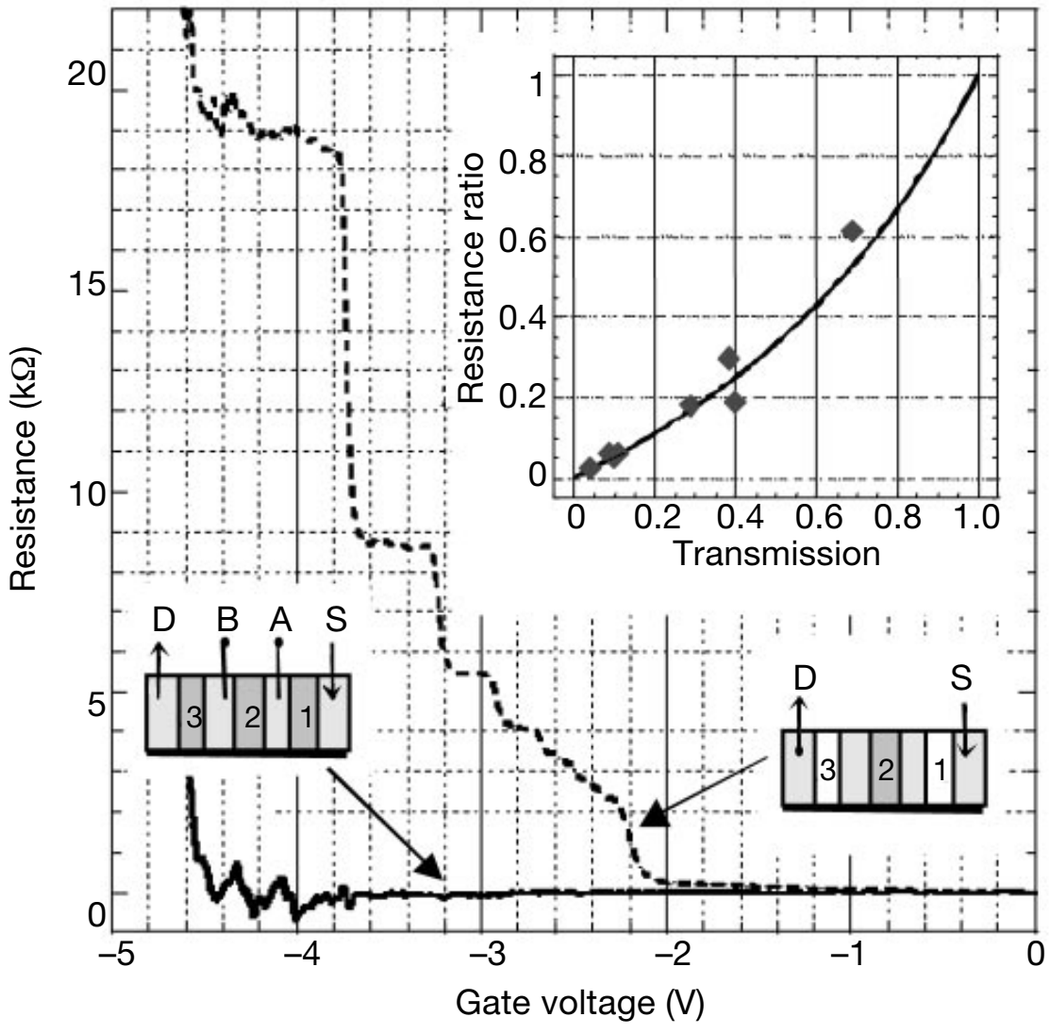

Figure 2 Two- and four-terminal resistances of a ballistic quantum wire. The dashed line shows the two-terminal resistance of the 2-μm-long central section of the wire versus the voltage applied to the associated gate 2. Gates 1 and 3 are not activated. The solid line shows the four-terminal resistance, $(V_A - V_B)/I$, versus the voltage applied to gate 2. Here V_A and V_B are the voltages at probes A and B respectively and I is the current driven from source to drain. For this measurement, the voltages applied to gates 1 and 3 correspond to a single mode in the wire sections in front of these gates. Measurements were performed at a temperatureof $\theta = 300$ mK with an excitation current smaller than 1 nA. While the two-terminal resistance moves through the characteristic quantized resistance steps, the four-terminal resistance fluctuates around zero indicating that the inherent resistance of a clean one-dimensional wire is vanishingly small. The small oscillations around zero resistance (from –3.8V to –4.5V) suggest that mesoscopic variation of the various transmission amplitudes with the one-dimensional density dominate the resistance in this regime. Indeed a similar, although not identical, pattern is observed upon successive cool-downs of the same device. As expected, similar mesoscopic variations are observed when a magnetic field is applied (see Fig. 3). Inset, probe invasiveness in a quantum wire. Diamonds, the ratio between the four-terminal and two-terminal resistances versus the invasiveness of the voltage probes (see text). Solid line, theoretical prediction of the Landauer–Buttiker model[16] (see text). All measurements are for single-mode wires.

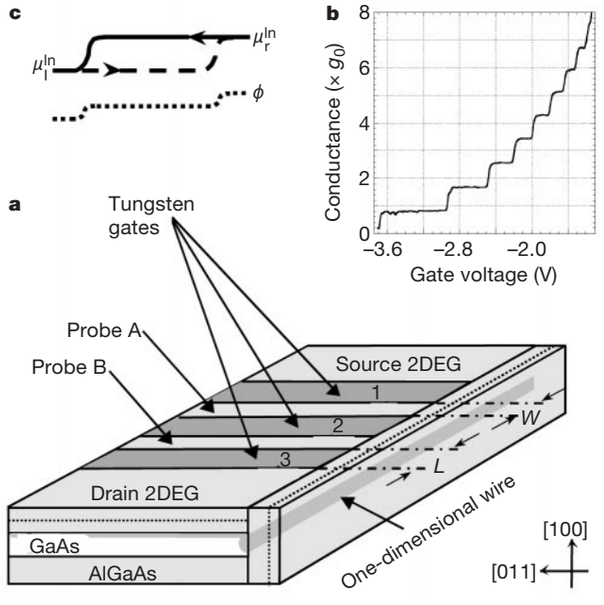

Coherence length

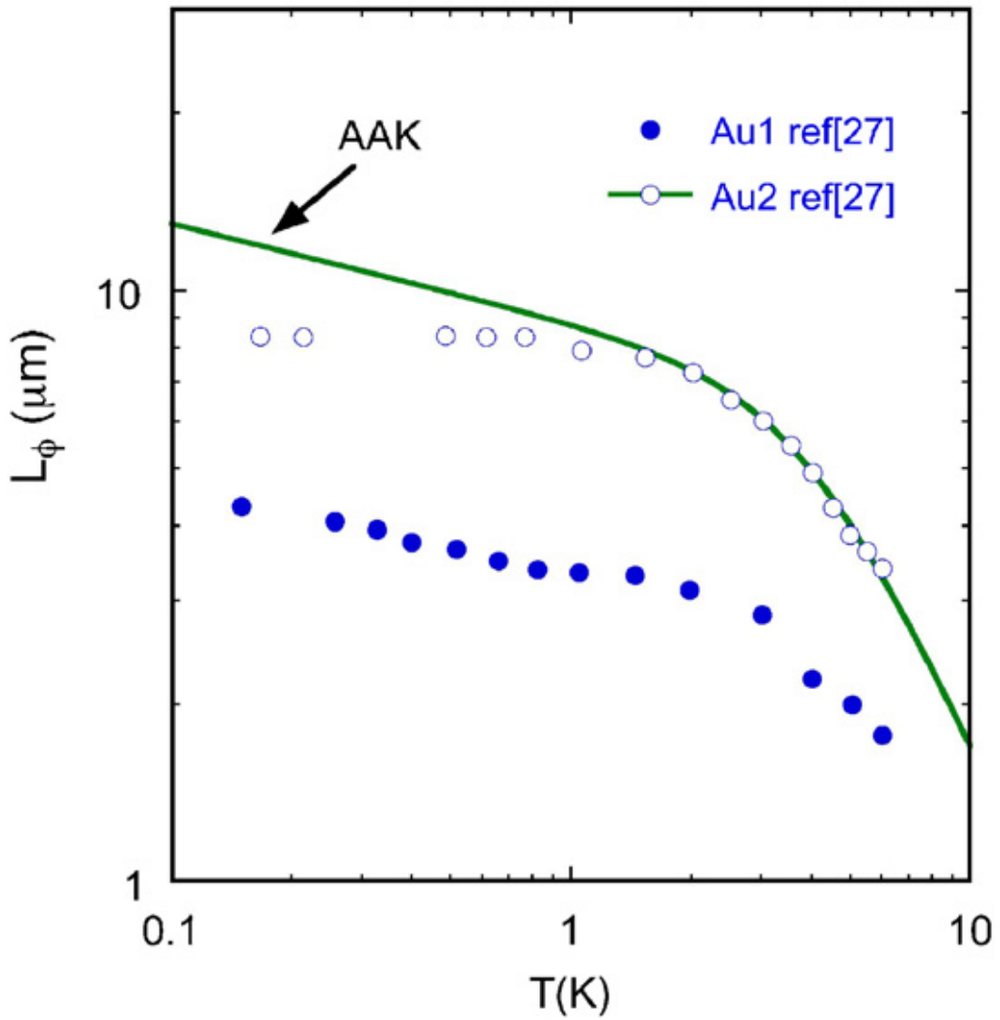

Fig. 1. Phase coherence length as a function of temperature for an ultra-pure gold sample before (•) and after (○) annealing. The solid line corresponds to the theoretical expectation within the AAK picture [30]. Data are taken from Ref. [26].

Weak localisation in a Cr wire

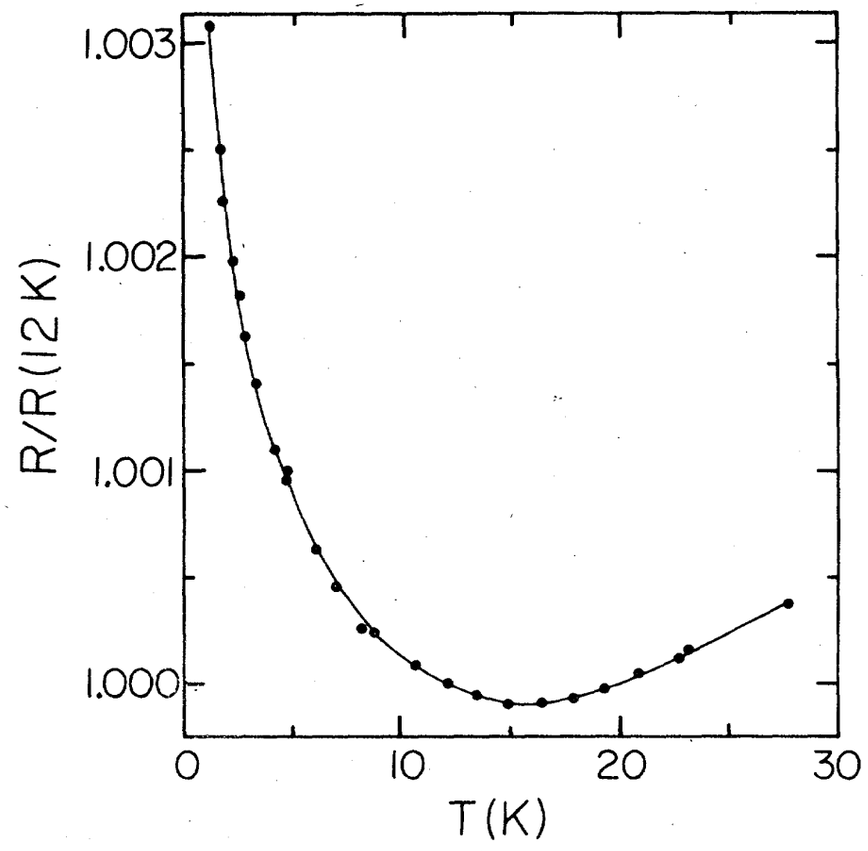

FIG. 7. Resistance as a function of temperature for a dirty wire with $\sqrt{A} = 890$ Å. $R(12\ \mathrm{K}) = 58\ \mathrm{k}\Omega$.

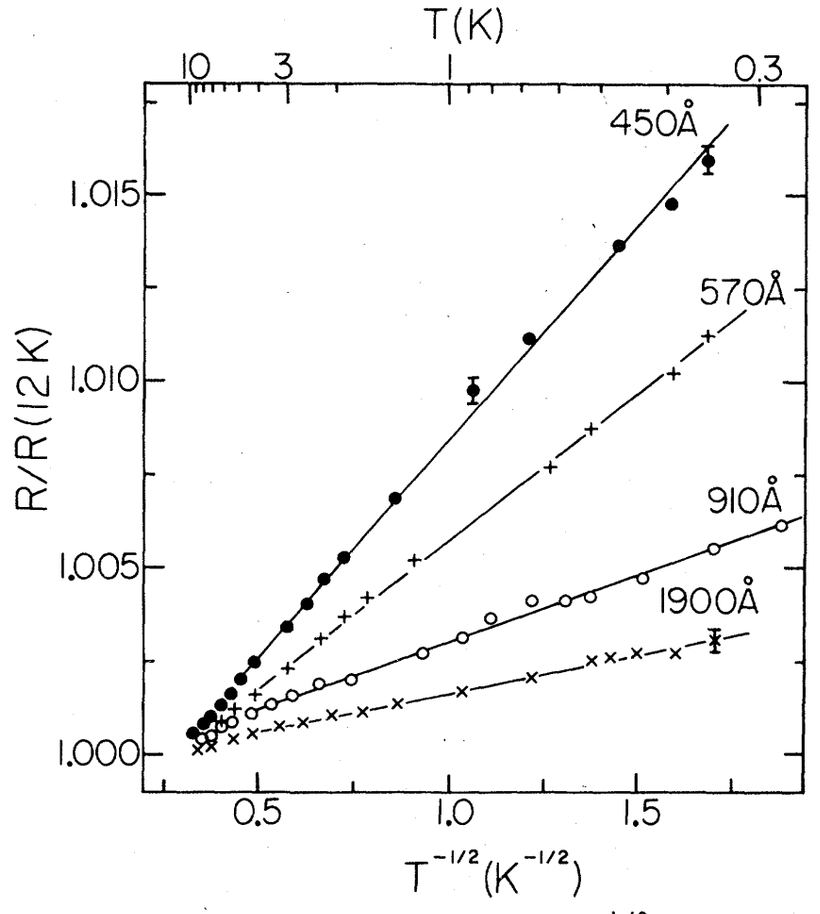

FIG. 10. Resistance as a function of $T^{-1/2}$ for several dirty wires. The data are the same as that shown in Fig. 8. For the sake of clarity some overlapping points have been omitted.

$$\Delta R \propto l_\phi \propto T^{-1/2}$$

Aharonov-Bohm effect in a metallic ring

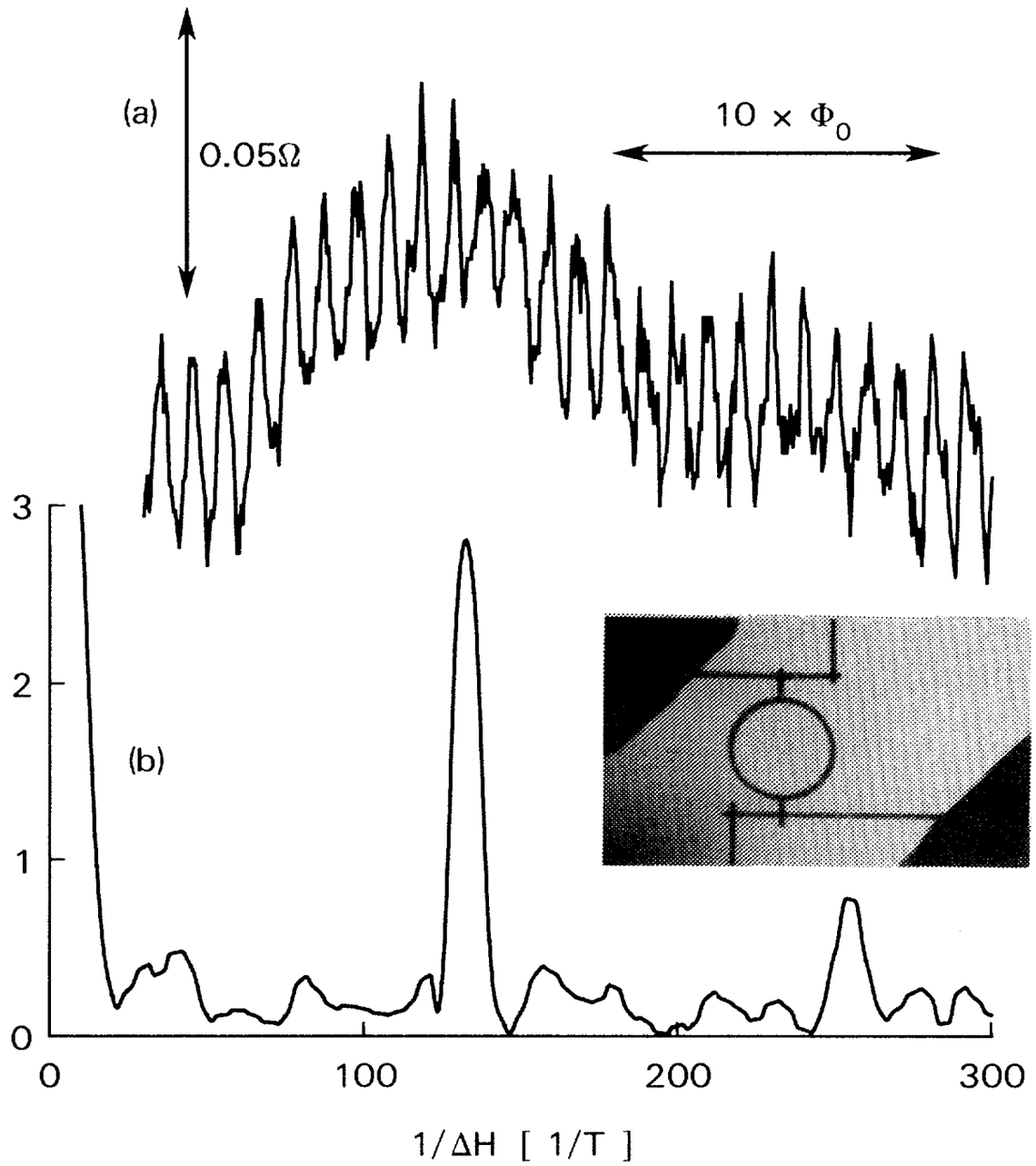

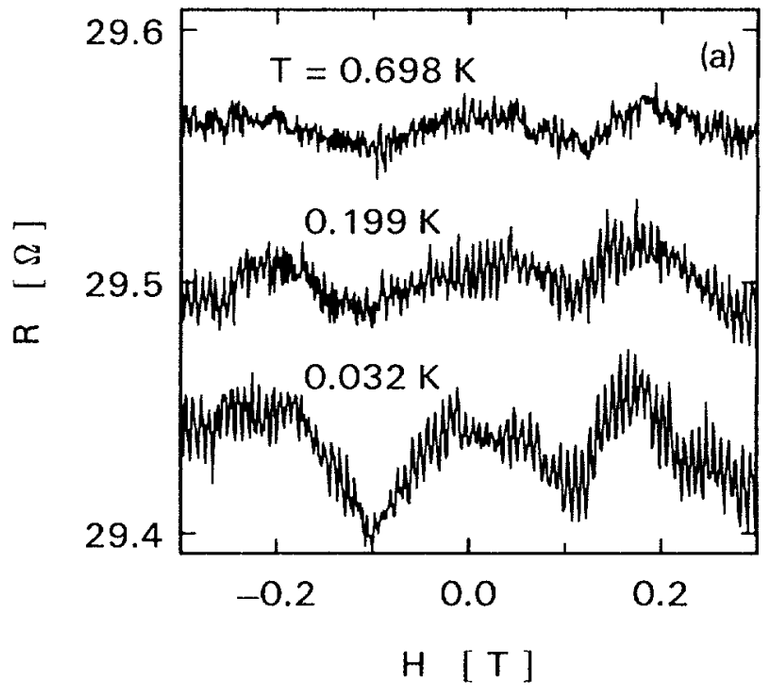

FIG. 1. (a) Magnetoresistance of the ring measured at $T = 0.01$ K. (b) Fourier power spectrum in arbitrary units containing peaks at h/e and $h/2e$. The inset is a photograph of the larger ring. The inside diameter of the loop is 784 nm, and the width of the wires is 41 nm.

Weak localisation in a topological insulator (Bi_2Te_2Se)

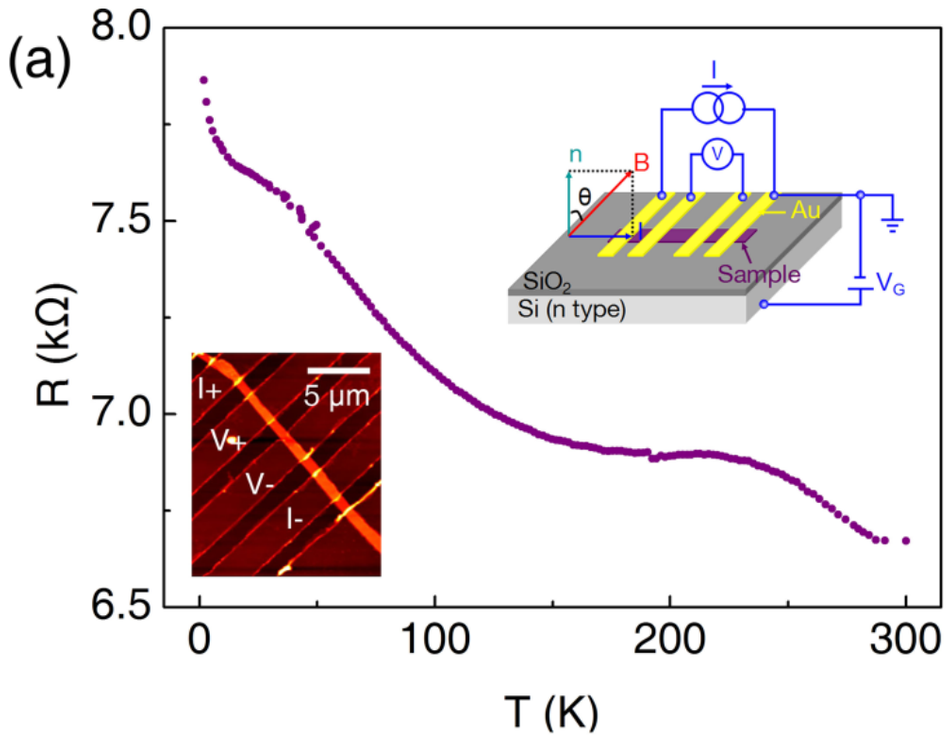

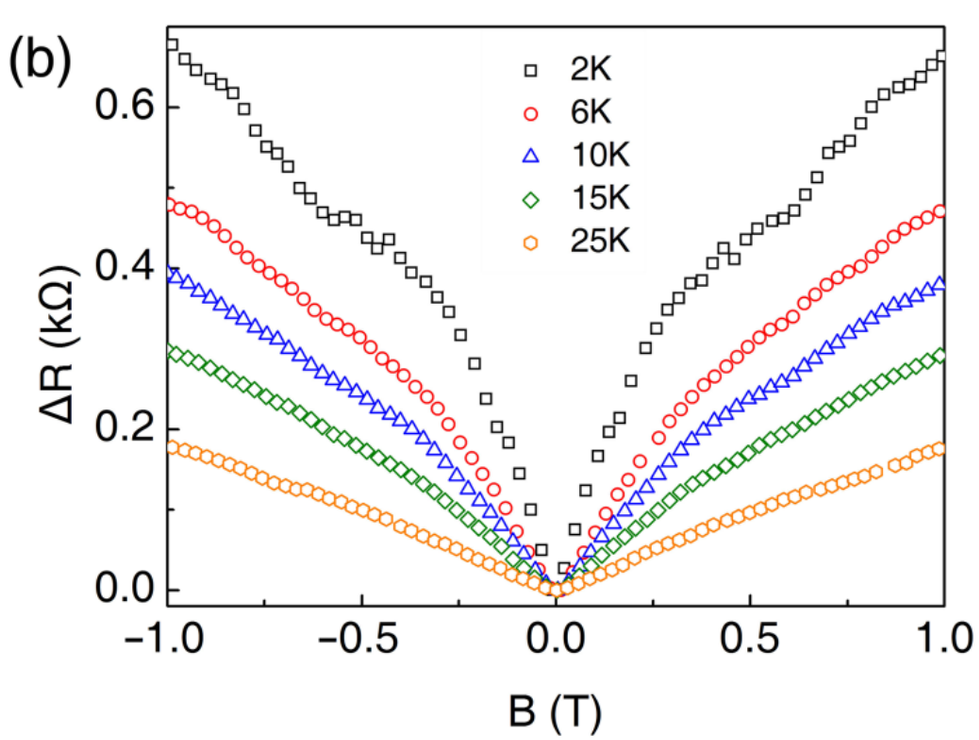

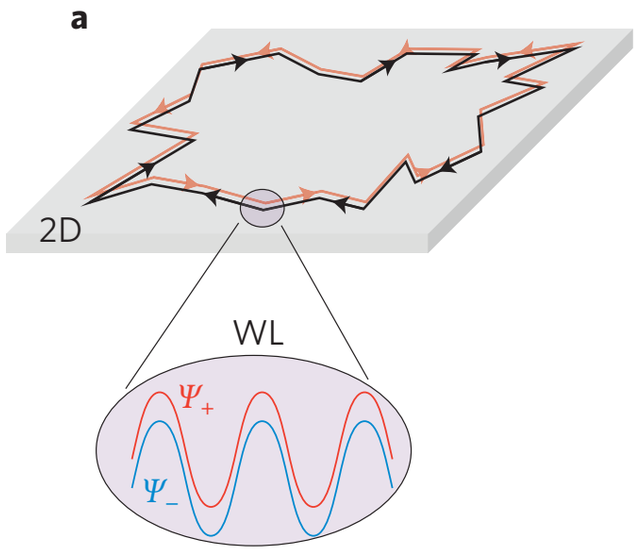

Relationship between R(B) and coherence time

$$\kappa \equiv \left.\frac{\partial^2 \sigma}{\partial B_\perp^2}\right|_{B_\perp=0} = \frac{16\pi}{3}\frac{e^2}{h}\left(\frac{D\tau_\varphi}{h/e}\right)^2$$